A NEW RFQ MODEL AND SYMPLECTIC MULTI-PARTICLE TRACKING IN THE IMPACT CODE SUITE*

J. Qiang†, Lawrence Berkeley National Laboratry, Berkeley, USA
Z. Wang, H. P. Li, Peking University, Beijing, China

Abstract

The IMPACT code suite is a self-consistent parallel three-dimensional beam dynamics simulation toolbox that combines the magnetic optics method and the parallel particle-in-cell method. It has been widely used to study high intensity/high brightness beams in many accelerators. In this paper, we will report on recent improvements to the code such as the capability to model RFQ in time domain and symplectic multi-particle tracking with a gridless spectral solver for space-charge simulation.

INTRODUCTION

The IMPACT code suite is a parallel three-dimensional multi-particle tracking code to simulate charged particle beam dynamics in high intensity/high brightness accelerators. It includes a time-dependent code, IMPACT-T [1] and a longitudinal position dependent code, IMPACT [2]. Both codes use a particle-in-cell (PIC) method to self-consistently model the space-charge effects in the simulation. It has been used to model high intensity proton/ion linac, high brightness photoinjector, electron linac, proton synchrotron and other accelerators.

A NEW RFQ MODEL

The popular RFQ design code Parmteqm uses position as an independent variable and has a two-dimensional space-charge solver [3]. These approximations might introduce significant errors at lower energy for high intensity proton/ion beams. A new RFQ model is added into the IMPACT-T code with a three-dimensional space-charge solver including space charge effects within the bunch and the effects from neighboring bunches. In the RFQ model, eight term expression was implemented to account for the external accelerating/focusing effects. All coefficients can be obtained from the Parmteqm output file PARIOUT.OUT. Normally, an RFQ consists of different types of cells including radial matching section (RMS) cells, normal cells, and transition cells (including $m = 1$ cell and fringe cell). Inside the normal cells, the potential expression is given by

$$\begin{aligned} U(r,\theta,z) = \frac{V}{2}\{&A_{01}(\frac{r}{r_0})^2\cos(2\theta) + A_{03}(\frac{r}{r_0})^6\cos(6\theta) \\ &+[A_{10}I_0(kr) + A_{12}I_4(kr)\cos(4\theta)]\cos(kz) \\ &+[A_{21}I_2(2kr)\cos(2\theta) + A_{23}I_6(2kr)\cos(6\theta)]\cos(2kz) \\ &+[A_{30}I_0(3kr) + A_{32}I_4(3kr)\cos(4\theta)]\cos(3kz)\} \end{aligned} \quad (1)$$

In the above equation, $0 \le z \le L$, where L is the length of a cell. In the sine and cosine terms, $k = \pi/L$; in the modified Bessel function $I_{2m}(nkr)$ terms, k varies linearly over the cell. In the fringe cell and the RMS cells, the potential expression is given by

$$\begin{aligned} U(r,\theta,z) = &\frac{V}{2}\frac{6A_{01}}{k^2r_0^2}(I_2(kr)\cos(kz) + \frac{1}{27}I_2(3kr) \\ &\cos(3kz))\cos(2\theta) \end{aligned} \quad (2)$$

where $k = \pi/(2L)$, L is length of transition cell. In the transition cell, the potential expression is given by

$$\begin{aligned} U(r,\theta,z) = &\frac{V}{2}[(\frac{r}{r_0})^2\cos(2\theta) - A_{10}I_0(kr)\cos(kz) \\ &-A_{30}I_0(3kr)\cos(3kz)] \end{aligned} \quad (3)$$

where $k = \pi/(2L)$, L is the length of the transition cell. In all of these expressions, the $A_{01}, \cdots, A_{32}$ coefficients values can be calculated by linear interpolation at each z (defining $z = 0$ at the interface).

As an illustration of this new model, we simulated a charged proton beam with 5 mA current at 2.1 MeV transporting through an RFQ designed for the PIP-II project. The final beam phase space distributions at the RFQ exit from the IMPACT-T simulation, from the Toutatis [4] simulation, and from the ParmteqM simulation are shown in Fig. 1. It is seen that the IMPACT-T results agree with the Toutatis and the Parmteqm simulation results quite well.

SYMPLECTIC MULTI-PARTICLE TRACKING WITH A GRIDLESS SPECTRAL METHOD

In the accelerator beam dynamics simulation, for a multi-particle system with N_p charged particles subject to both space-charge self fields and external fields, the approximate Hamiltonian of the system can be written as:

$$H = \sum_i \mathbf{p}_i^2/2 + \frac{1}{2}\sum_i\sum_{j,j\neq i} q\phi(\mathbf{r}_i,\mathbf{r}_j) + \sum_i q\psi(\mathbf{r}_i) \quad (4)$$

where $H(\mathbf{r}_1,\mathbf{r}_2,\cdots,\mathbf{p}_1,\mathbf{p}_2,\cdots,s)$ denotes the Hamiltonian of the system, ϕ is the space-charge Coulomb interaction potential among the charged particles (with appropriate boundary conditions), ψ denotes the potential associated with the external fields. $\mathbf{r}_i$ denotes the canonical spatial coordinates of particle i, and $\mathbf{p}_i$ the normalized canonical momentum coordinates of the particle i. The equations governing the motion of individual particle i follows the Hamilton's equa-

* Work supported by the U.S. Department of Energy under Contract No. DE-AC02-05CH11231.
† jqiang@lbl.gov

ISBN 978-3-95450-178-6

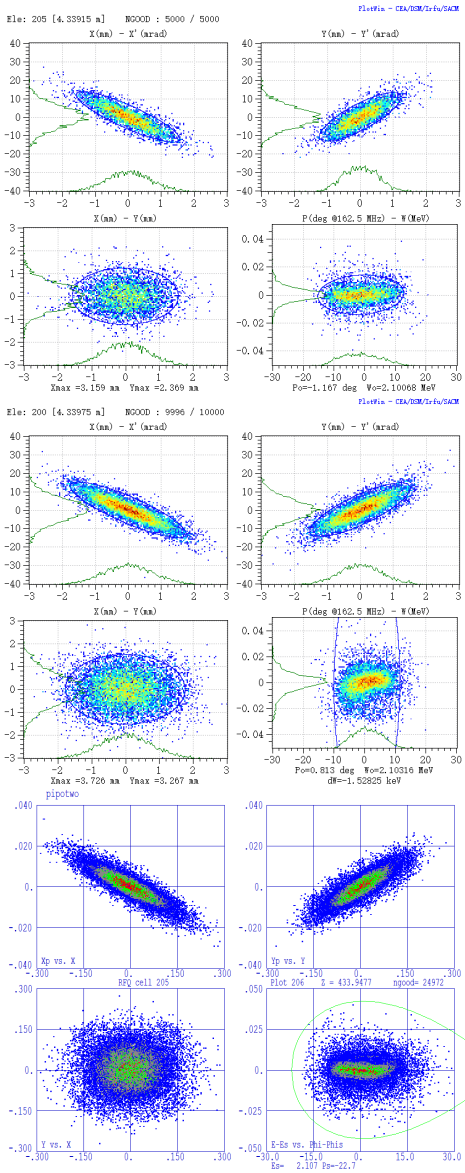

Figure 1: Beam phase space at the RFQ exit from the IMPACT-T simulation (top), from the Toutatis (middle), and from the Parmteqm simulation (bottom).

tions as:

$$\frac{d\mathbf{r}_i}{ds} = \frac{\partial H}{\partial \mathbf{p}_i} \quad (5)$$

$$\frac{d\mathbf{p}_i}{ds} = -\frac{\partial H}{\partial \mathbf{r}_i} \quad (6)$$

Let ζ denote the 6N-vector of coordinates, the above Hamilton's equation can be rewritten as:

$$\frac{d\zeta}{ds} = -[H, \zeta] \quad (7)$$

where [,] denotes the Poisson bracket. A formal solution for above equation after a single step τ can be written as:

$$\zeta(\tau) = \exp(-\tau(: H :))\zeta(0) \quad (8)$$

Here, we have defined a differential operator $: H :$ as $: H : g = [H, g]$, for arbitrary function g, and assumed H is not an explicit function of s [1]. For a Hamiltonian that can be written as a sum of two terms $H = H_1 + H_2$, an approximate solution to above formal solution can be written as [6]

$$\begin{aligned}\zeta(\tau) &= \exp(-\tau(: H_1 : + : H_2 :))\zeta(0) \\ &= \exp(-\frac{1}{2}\tau : H_1 :)\exp(-\tau : H_2 :) \\ &\quad \exp(-\frac{1}{2}\tau : H_1 :)\zeta(0) + O(\tau^3)\end{aligned} \quad (9)$$

Let $\exp(-\frac{1}{2}\tau : H_1 :)$ define a transfer map $\mathcal{M}_1$ and $\exp(-\tau : H_2 :)$ a transfer map $\mathcal{M}_2$, for a single step, the above splitting results in a second order numerical integrator to the original Hamilton equation as:

$$\begin{aligned}\zeta(\tau) &= \mathcal{M}(\tau)\zeta(0) \\ &= \mathcal{M}_1(\tau/2)\mathcal{M}_2(\tau)\mathcal{M}_1(\tau/2)\zeta(0)\end{aligned} \quad (10)$$

Using the above transfer maps $\mathcal{M}_1$ and $\mathcal{M}_2$, higher order numerical integrator can also be constructed [6, 7].

The above numerical integrators Eq. 10 will be symplectic if both the transfer map $\mathcal{M}_1$ and the transfer map $\mathcal{M}_2$ are symplectic. A transfer map $\mathcal{M}_i$ is symplectic if and only if the Jacobian matrix M_i of the transfer map $\mathcal{M}_i$ satisfies the condition:

$$M_i^T J M_i = J \quad (11)$$

where J denotes the $6N \times 6N$ matrix given by:

$$J = \begin{pmatrix} 0 & I \\ -I & 0 \end{pmatrix} \quad (12)$$

and I is the $3N \times 3N$ identity matrix.

For the given Hamiltonian in Eq. 4, we can choose H_1 as:

$$H_1 = \sum_i \mathbf{p}_i^2/2 + \sum_i q\psi(\mathbf{r}_i) \quad (13)$$

Standard charged optics methods can be used to find a symplectic transfer map $\mathcal{M}_1$ for this Hamiltonian with the external field from most accelerator beam line elements [8].

We can choose H_2 as:

$$H_2 = \frac{1}{2}\sum_i \sum_j q\phi(\mathbf{r}_i, \mathbf{r}_j) \quad (14)$$

which is only a function of positions, i.e. $H_2(\mathbf{r})$. The single step transfer map $\mathcal{M}_2$ can be written as:

$$\mathbf{r}_i(\tau) = \mathbf{r}_i(0) \quad (15)$$

$$\mathbf{p}_i(\tau) = \mathbf{p}_i(0) - \frac{\partial H_2(\mathbf{r})}{\partial \mathbf{r}_i}\tau \quad (16)$$

The Jacobi matrix of the above transfer map $\mathcal{M}_2$ is

$$M_2 = \begin{pmatrix} I & 0 \\ L & I \end{pmatrix} \quad (17)$$

[1] For the case that H is an explicit function of s, one can extend the variable space and a similar solution can still be obtained [5].

ISBN 978-3-95450-178-6

where L is a $3N \times 3N$ matrix. For M_2 to satisfy the symplectic condition Eq. 11, the matrix L needs to be a symmetric matrix, i.e.

$$L = L^T \tag{18}$$

Given the fact that $L_{ij} = \partial \mathbf{p}_i(\tau)/\partial \mathbf{r}_j = -\frac{\partial^2 H_2(\mathbf{r})}{\partial \mathbf{r}_i \partial \mathbf{r}_j}\tau$, the matrix L will be symmetric as long as it is analytically calculated from the H_2. If both the transfer map $\mathcal{M}_1$ and the transfer map $\mathcal{M}_2$ are symplectic, the numerical integrator Eq. 10 for multi-particle tracking will be symplectic.

The space charge Coulomb potential in the Hamiltonian H_2 can be obtained from the solution of the Poisson equation. In the following, we consider a coasting beam in a rectangular conducting pipe. In this case, the two-dimensional Poisson's equation can be written as:

$$\frac{\partial^2 \phi}{\partial x^2} + \frac{\partial^2 \phi}{\partial y^2} = -\frac{\rho}{\epsilon_0} \tag{19}$$

where, ρ the charge density distribution of the beam, and ϵ_0 is the dielectric constant in vacuum. The boundary conditions for the electric potential in the rectangular perfect conducting pipe are:

$$\phi(x = 0, y) = 0 \tag{20}$$
$$\phi(x = a, y) = 0 \tag{21}$$
$$\phi(x, y = 0) = 0 \tag{22}$$
$$\phi(x, y = b) = 0 \tag{23}$$

where a is the horizontal width of the pipe and b is the vertical width of the pipe.

Given the boundary conditions in Eq. 20-23, the electric potential ϕ and the source term ρ can be approximated using two sine functions as [9–12]:

$$\rho(x, y) = \sum_{l=1}^{N_l} \sum_{m=1}^{N_m} \rho^{lm} \sin(\alpha_l x) \sin(\beta_m y) \tag{24}$$

$$\phi(x, y) = \sum_{l=1}^{N_l} \sum_{m=1}^{N_m} \phi^{lm} \sin(\alpha_l x) \sin(\beta_m y) \tag{25}$$

where

$$\rho^{lm} = \frac{4}{ab} \int_0^a \int_0^b \rho(x, y) \sin(\alpha_l x) \sin(\beta_m y)\, dxdy \tag{26}$$

$$\phi^{lm} = \frac{4}{ab} \int_0^a \int_0^b \phi(x, y) \sin(\alpha_l x) \sin(\beta_m y)\, dxdy \tag{27}$$

where $\alpha_l = l\pi/a$ and $\beta_m = m\pi/b$. The above approximation follows a numerical spectral Galerkin method since each basis function satisfies the transverse boundary conditions on the wall. For a smooth analytical function, this spectral approximation has an accuracy with the numerical error that scales as $O(\exp(-cN))$ with $c > 0$ and N is the order of the basis function used in the approximation. Substituting above expansions into the Poisson equation and making use of the orthonormal conditions of the sine functions, we obtain

$$\phi^{lm} = \frac{\rho^{lm}}{\epsilon_0 \gamma_{lm}^2} \tag{28}$$

where $\gamma_{lm}^2 = \alpha_l^2 + \beta_m^2$.

In the multi-particle tracking, the charge density $\rho(x, y)$ can be represented by:

$$\rho(x, y) = \sum_{j=1}^{N_p} w \delta(x - x_j) \delta(y - y_j) \tag{29}$$

where w is the charge weight of each individual particle and δ is the Dirac function. Using Eq. 26 and Eq. 28, we obtain:

$$\phi^{lm} = \frac{1}{\epsilon_0 \gamma_{lm}^2} \frac{4}{ab} w \sum_j \sin(\alpha_l x_j) \sin(\beta_m y_j) \tag{30}$$

and the potential as:

$$\phi(x, y) = \frac{1}{\epsilon_0} \frac{4}{ab} w \sum_j \sum_l \sum_m \frac{1}{\gamma_{lm}^2} \sin(\alpha_l x_j) \sin(\beta_m y_j) \sin(\alpha_l x) \sin(\beta_m y) \tag{31}$$

Now, the Hamiltonian H_2 can be written as:

$$H_2 = \frac{1}{2\epsilon_0} \frac{4}{ab} w \sum_i \sum_j \sum_l \sum_m \frac{1}{\gamma_{lm}^2} \sin(\alpha_l x_j) \sin(\beta_m y_j) \sin(\alpha_l x_i) \sin(\beta_m y_i) \tag{32}$$

The one-step symplectic transfer map $\mathcal{M}_2$ of a particle i for this Hamiltonian is given as:

$$p_{xi}(\tau) = p_{xi}(0) - \tau \frac{1}{\epsilon_0} \frac{4}{ab} w \sum_j \sum_l \sum_m \frac{\alpha_l}{\gamma_{lm}^2} \sin(\alpha_l x_j) \sin(\beta_m y_j) \cos(\alpha_l x_i) \sin(\beta_m y_i) \tag{33}$$

$$p_{yi}(\tau) = p_{yi}(0) - \tau \frac{1}{\epsilon_0} \frac{4}{ab} w \sum_j \sum_l \sum_m \frac{\beta_m}{\gamma_{lm}^2} \sin(\alpha_l x_j) \sin(\beta_m y_j) \sin(\alpha_l x_i) \cos(\beta_m y_i) \tag{34}$$

Using a symplectic transfer map $\mathcal{M}_1$ for external field Hamiltonian H_1 from some charged particle optics code and following Eq. 10, one obtain a symplectic multi-particle tracking model including self-consistent space-charge effects.

As an illustration of above symplectic multi-particle tracking model, we simulated a 1 GeV coasting proton beam transporting through a rectangular conducting pipe with a FODO lattice for transverse focusing. The initial transverse density distribution is a Gaussian distribution and given in Fig. 2. We computed the electric field along x axis using above direct gridless spectral solver with 15×15 modes and the electric field from a 2nd order finite difference solver with 129×129 grid points. The results are shown in Fig. 3. The solution of the spectral solver agrees with the finite difference solver very well even with 15×15 modes due to the fast convergence property of the spectral method.

Figure 4 shows the proton beam root-mean-square (rms) envelope evolution through 20 FODO lattice periods. The FODO lattice used in this example consists of two quadupoles and three drifts in a single period. The total length of the period is 1 meter. The 0 current phase advance

ISBN 978-3-95450-178-6

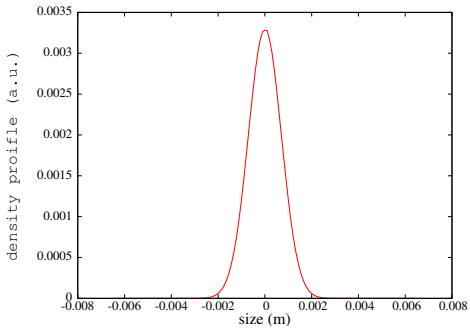

Figure 2: Charge density distribution along x axis.

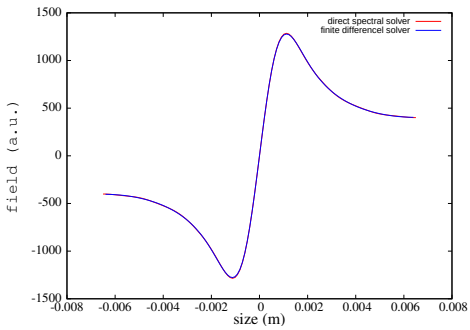

Figure 3: Electric field on x axis from the above direct spectral solver (red) and from the 2nd order finite difference solver (green).

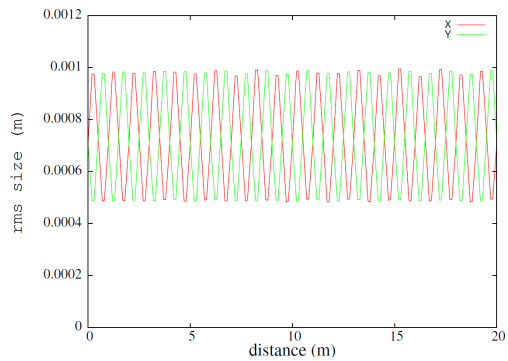

Figure 4: RMS envelope evolution of the beam.

is about 87 degrees and the phase advance with current is about 74 degrees.

The symplectic integrator is normally used for long term tracking since it helps preserve phase space structure during the numerical integration. Figures 5 shows stroboscopic plots (every 10 periods) of $x - p_x$ and $y - p_y$ phase space evolution of a test particle through 100, 000 lattice periods including the self-consistent space-charge forces. As a comparison, we also show in this plot the phase space evolution of the same initial test particle using the standard momentum conservation particle-in-cell (PIC) method with a 2nd order finite difference solver for space-charge calculation. In general, the two models show similar shapes in phase space. However, looking into the details of the phase space, the two models show quite different structures. The single

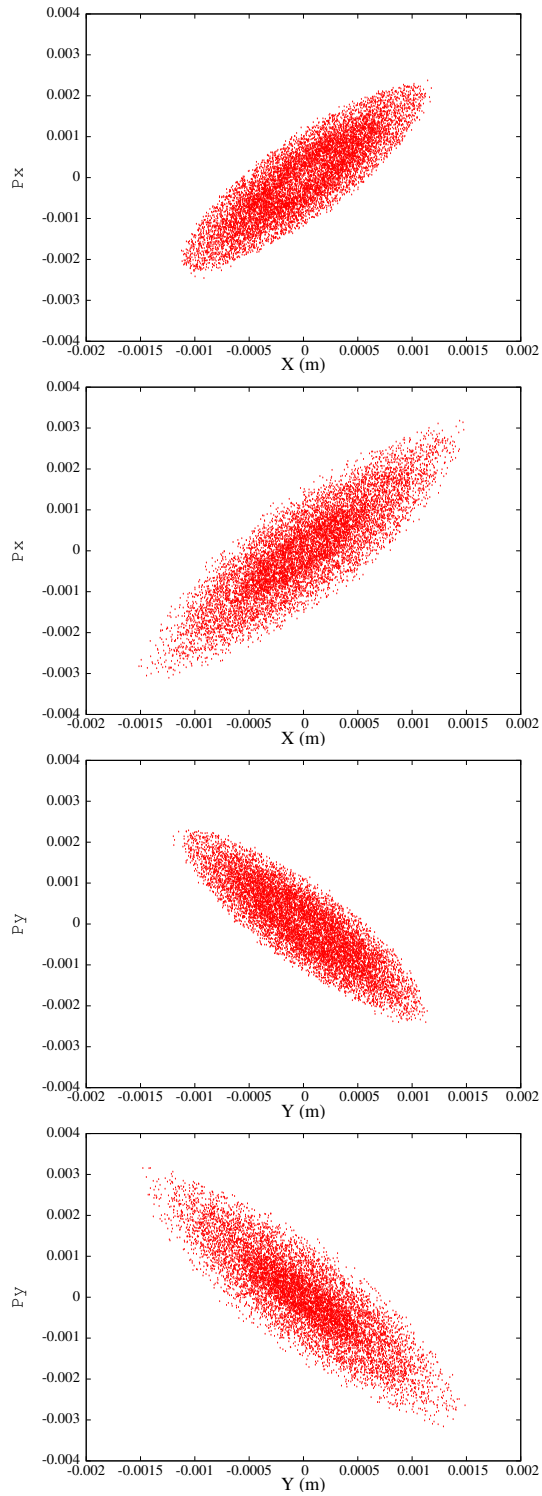

Figure 5: Stroboscopic plot (every 10 periods) of phase space evolution of a test particle from the symplectic-spectral model (top and 3rd) and from the PIC-finite difference model (2nd and bottom).

particle phase space from the PIC model shows a dense core while the symplectic multi-particle model shows a nearly hollow core. Figure 6 shows the 4-dimensional emittance growth evolution from the symplectic model and from the

ISBN 978-3-95450-178-6

PIC model. It is seen that the symplectic model shows a much smaller emittance growth than the PIC model does. This emittance growth is a numerical artifact due to the small number of macroparticles (50, 000) used in the simulation.

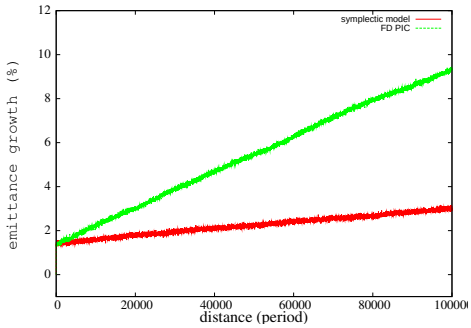

Figure 6: Four dimensional emittance growth evolution from the symplectic multi-particle spectral model (red) and from the PIC finite difference model(green).

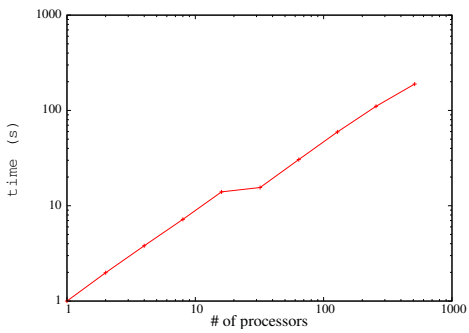

Figure 7: Parallel speedup of the symplectic tracking model on a Cray XC30 computer.

The symplectic multi-particle model with a gridless spectral solver can be used for long-term tracking study including space-charge effects. However, the computational complexity of the model scales as $O(N_l \times N_m \times N_p)$. The standard PIC model can have a computational cost of $O(N_p)+O(N_{grid}logN_{grid})$ when an efficient Poisson solver is used. This suggests that the PIC model should be faster than the symplectic multi-particle model on a single processor. However, the symplectic multi-particle model can be very easily parallelized on a multi-processor computer. One can distribute the macroparticles uniformly across all processors to achieve a perfect load balance. By using a spectral method with exponentially decreasing errors, the number of modes $N_l \times N_m$ can be kept within a relatively small number, which significantly improves the computing speed. Figure 7 shows the parallel speed up of the symplectic multi-particle tracking model as a function of the number of processors for a fixed problem size, i.e. 50, 000 particles and 15×15 modes. It is seen that the model has an almost linear scaling up to 500 processors. This shows that the symplectic multi-particle spectral tracking model can have a good scalability on parallel computers.

CONCLUSION

In this paper, we have shown two improvements to the IMPACT code suite. The new time-dependent RFQ model with 3D space-charge solver enables the IMPACT code suite to simulate low energy high intensity proton/ion beam through an RFQ. The new symplectic multi-particle spectral model also enables the code for long term tracking including space-charge effects.

ACKNOWLEDGEMENTS

We would like to thank Dr. D. Li for the PIP-II RFQ Parmteqm inputs and Drs. G. Franchetti, F. Kesting, C. Mitchell for discussions. This research used computer resources at the National Energy Research Scientific Computing Center.

REFERENCES

[1] J. Qiang, S. Lidia, R. D. Ryne, and C. Limborg-Deprey, *Phys. Rev. ST Accel. Beams* **9**, 044204, 2006.

[2] J. Qiang, R. D. Ryne, S. Habib, V. Decyk, *J. Comput. Phys.* **163**, 434, 2000.

[3] K. R. Crandall *et al.*, LANL Technical Report No. LA-UR-96-1836, 1997.

[4] R. Duperrier, *Phys. Rev. ST Accel. Beams* **3**, 124201, 2000.

[5] E. Forest, "Beam Dynamics: A New Attitude and Framework," *The Physics and Technology of Particle and Photon Beams*, Vol. 8 (Harwood Academic Publishers, Amsterdam, 1998).

[6] E. Forest and R. D. Ruth, *Physica D* **43**, p. 105, 1990.

[7] H. Yoshida, *Phys. Lett.* A **150**, p. 262, 1990.

[8] R. D. Ryne, "Computational Methods in Accelerator Physics," US Particle Accelerator class note, 2012.

[9] D. Gottlieb and S. A. Orszag, *Numerical Analysis of Spectral Methods: Theory and Applications*, Society for Industrial and Applied Mathematics, 1977.

[10] J. Boyd, *Chebyshev and Fourier Spectral Methods*, Dover Publications, Inc. 2000.

[11] J. Qiang and R. D. Ryne, *Comp. Phys. Comm.* **138**, p. 18, 2001.

[12] J. Qiang, *Comp. Phys. Comm.* **203**, p. 122, 2016.

ISBN 978-3-95450-178-6